Assimilating a Time-Domain Representation of a Wave Energy Converter Into a Spectral Wave Model

Conference Paper · June 2016

DOI: 10.1115/OMAE2016-54235

5 authors, including:

Ewelina Luczko
University of Victoria
5 PUBLICATIONS **40** CITATIONS
SEE PROFILE

Helen Bailey
University of Victoria
23 PUBLICATIONS **254** CITATIONS
SEE PROFILE

Bryson Robertson
Oregon State University
75 PUBLICATIONS **1,389** CITATIONS
SEE PROFILE

Clayton E. Hiles
Kerr-Wood-Leidal Consulting Engineers
17 PUBLICATIONS **318** CITATIONS
SEE PROFILE

Proceedings of the ASME 2016 35th International Conference on Ocean, Offshore and Arctic Engineering
OMAE2016
June 19-24, 2016, Busan, South Korea

OMAE2016-54235

ASSIMILATING A TIME-DOMAIN REPRESENTATION OF A WAVE ENERGY CONVERTER INTO A SPECTRAL WAVE MODEL

Ewelina Luczko
University of Victoria
Victoria, BC, Canada

Helen Bailey
University of Victoria
Victoria, BC, Canada

Bryson Robertson
University of Victoria
Victoria, BC, Canada

Clayton Hiles
Cascadia Coast Research
Victoria, BC, Canada

Bradley Buckham
University of Victoria
Victoria, BC, Canada

ABSTRACT

To accommodate future power demands, wave energy converters (WECs) will be deployed in arrays, but largely unanswered questions of the annual energy production and environmental impact of such installations present regulatory dilemmas. In recent years, Sandia National Laboratories (SNL) has developed a modified version of the Simulating Waves Nearshore (SWAN) wave model to simulate WEC energy extraction in a propagating wave field. The SNL source code modifications to SWAN have facilitated a way to characterize the frequency dependent power absorption of a device in a spectral model using standard WEC parameterizations. The work presented in this paper seeks to build on source code modifications previously made by SNL. A new WEC meta-model, alters the incident wave spectrum based on power extracted from the sea and dissipated by hydrodynamic losses experienced at the WEC. These losses are calculated in an external six degree of freedom (DOF) time domain WEC simulation. The two WEC models were compared in terms of significant wave height reduction in the WEC's lee and annual power production. The new model reduced the estimated distance required for the waves to recover 95% of the incident wave height by 50% for the same sea state. A 4.5% difference in annual power production was observed for a WEC operating in the lee of another device when deployed off the west coast of Canada.

NOMENCLATURE

$A(\infty)$	=	*added mass matrix at infinite freq.*	kg
B	=	*radiation damping matrix*	kg/s
C	=	*hydrostatic coefficient matrix*	kg/s^2
E	=	*energy density*	m^2/Hz
F_m	=	*force from the mooring*	N
F_{PTO}	=	*force from the PTO*	N
F_v	=	*force from viscous drag*	N
H_s	=	*significant wave height*	m
J	=	*wave energy flux*	W/m
K_t^2	=	*transmission coefficient*	-
M	=	*global mass matrix*	kg
P_{abs}	=	*power absorbed*	W
P_{inc}	=	*incident power*	W
PWL	=	*power with losses*	-
RCW	=	*relative capture width*	-
T_e	=	*energy period*	s
T_p	=	*peak period*	s
η	=	*water surface elevation*	m
i	=	*frequency bin index*	-
c_g	=	*group velocity*	m/s
g	=	*gravitational constant*	m/s^2
$k(t)$	=	*radiation impulse response function*	-
ρ	=	*density of water*	kg/m^3
σ	=	*frequency*	Hz
θ	=	*direction*	rad

INTRODUCTION

The implementation of Wave Energy Converters (WECs) on a large scale faces many obstacles due to a number of unanswered regulatory questions. These questions can only be resolved when the benefits (i.e. energy yield) and the costs (i.e. coastal ecological impacts) of this emerging technology are well defined. Several works have described computational modeling techniques for a single WEC [1]–[6], and these methods show great promise for estimating the performance of an individual device. To model the performance of WEC arrays a modified wave field must be calculated for each WEC in an array based on the power extracted and dissipated by the preceding WECs. While the collective array power production is a valuable objective in such a modeling exercise, an added

benefit is a depiction of the WEC array's impact on the near shore wave circulation.

To help address the WEC array modeling problem, Sandia National Laboratories (SNL) is developing a modified version of the Simulating Waves Nearshore (SWAN) wave model which includes the effect of WEC energy extraction on the propagating wave field [7] [1]. Three versions of the SNL-SWAN code have been released to date relying on a condensed representation of a WEC's power production characteristics through a WEC meta-model. The present work proposes a change in the structure of this WEC meta-model with a goal of improving the fidelity of the WEC farm representation in the SNL-SWAN software. A validation of the new meta-model framework cannot be included in the scope of the current work. Rather, the sensitivity of WEC array power production estimates to the proposed changes is established.

The WEC considered in this work is a Backwards Bent Duct Buoy (BBDB), a type of floating Oscillating Water Column WEC. A high fidelity six DOF WEC time domain simulator is used to investigate the major mechanisms of power loss inside the WEC power conversion process. The WEC simulations include power-take-off, wave/WEC interactions and mooring dynamics. Using the simulation outputs from the time domain model, a novel WEC representation has been created for use within SNL-SWAN. This novel parameterization is employed to determine the WEC's impact on the wave climate as well as power produced by the device.

This investigation commences with a non-exhaustive review of models formerly used to characterize WECs offshore. Potential flow, Boussinesq, mild slope and spectral models have all been used in an effort to quantify a device's impact on the nearshore. Secondly, an overview of the functionality within Sandia National Laboratory's (SNL) modified version of SWAN is presented. This review outlines the inputs required for each module and describes how the device's energy absorption is characterized. Thirdly, the operating principle behind the novel WEC module is introduced. To demonstrate the importance of this work, the BBDB OWC is used as a reference device in two test case configurations. The investigation is concluded with results, analysis, future work and limitations.

WEC ARRAY MODELLING

Investigations concerning the effect a WEC has on the surrounding wave climate have been conducted in the past primarily for array optimization. Early findings and similar methods have then been employed to determine the reduction in energy sustained at the coastline as a result of WEC array deployment. A number of approaches have been used to model WEC effects on the surrounding wave climate, some of which are outlined below [8]–[10].

POTENTIAL FLOW MODELS

Potential flow models characterize WECs in moderate sea states with results that agree well with CFD calculations as long as linearity assumptions are not violated. Previous work by de Backer et al. investigated two array layouts within a boundary element method (BEM) model under constrained and unconstrained conditions [11]. The power absorption of each row of the devices in the array was compared. Ricci et al. also investigated the power production of arrays by modelling point absorbers with varying geometries in a BEM solver [10]. Potential flow models have widely been applied in determining the array configuration which maximizes power but their use is limited to certain cases. Namely, in higher energy sea states, linearity assumptions are violated and viscous forces dominate. The application of these models to arrays is limited by the increased computational cost of every additional WEC. It is presently only feasible to model arrays of five to ten devices [9].

BOUSSINESQ MODELS

Phase-resolving Boussinesq models have also been used to characterize the impacts an array of WECs would have on the nearshore climate. Boussinesq models are based on the solution of a set of partial differential flow equations from which the vertical coordinate is omitted. Boussinesq models predict the nearshore hydrodynamic impact effectively on a small scale but are too computationally intensive for larger areas or longer periods of time [9]. An array of five interacting devices was modelled by Venugopal and Smith near the Orkney Islands, Scotland, using an enhanced Boussinesq solver [12]. The devices were modeled as both reflecting and absorbing sponge layers however, transmission and reflection coefficients were not related to specific devices. Phase resolved Boussinesq models are favorable for analyzing device interactions on a small scale but become cumbersome in larger spatial extents or longer time durations because of the computational cost of the model.

MILD SLOPE MODELS

Mild slope equations are a linearized form of the Boussinesq shallow water equations. These equations describe the transformation of linear irregular waves across a slowly changing bathymetry. Beels has studied the wake effects of a single device and array of overtopping WECs in a mild slope model in both uni- and multi-directional waves [13], [14]. Further work was conducted by Stratigaki where arrays were represented by a coupled BEM and mild slope model [15]. Most recently, Babarit et al. [16] characterized the far field effect of a device with a Kochin function found using the diffracted and radiated velocity potential calculated from a BEM solver. The radiated potential is perturbed based on the WEC dynamics at the given sea condition. The total far field potential is then converted to variance and input back into the resource model. Mild-slope models have a lower computational cost than Boussinesq models [9]. Both the Boussinesq and mild-slop equations solve for water surface elevation and account for horizontal and vertical flow velocity structures. These models are suitable candidates for resolving radiation and diffraction around wave energy converters.

[1] Releases to date: https://github.com/SNL-WaterPower/SNL-SWAN

However, the computational expense of these models limits their use to domains a few kilometres wide, smaller arrays of devices and shorter time durations [8]; for resource assessment studies, including estimation of WEC farm output, executed on large domains these models are compromised by slow execution speeds.

SPECTRAL ACTION DENSITY MODELS

Spectral models are phase-averaged wave propagation models where the spectral action density equation, as seen in Equation 1, is solved for each time step. The energy conservation equation allows for a quick and numerically stable solution to wave propagation along a shoreline. The model is capable of representing most wave nonlinearities such as wave breaking, bottom friction and wave-wave interactions [17]. Spectral phase-averaged models cannot explicitly model diffraction and thus employ numerical approximations such as the phase-decoupled refraction diffraction model [18]. The spectral approach is computationally less demanding than the previously mentioned approaches however fidelity is sacrificed as a result of this. Phase dependent interactions such as radiation cannot explicitly be modeled however will be approximated, as discussed later on.

Folley and Silverthorne represented WECs as source and sink terms within TOMAWAC, a spectral action density model developed at the Electricité de France's Studies and Research Division. Frequency-dependent reflection and absorption were characterized in these simulations by a device's hydrodynamic coefficients [8]. SWAN has also been used to model WEC arrays as both a single obstacle and a number of obstacles [9], using a transmission coefficient specifying the percentage of energy absorbed by the device [19], [20].

Recently, SNL-SWAN has improved the characterization of a WEC within a wave model by modifying the standard obstacle command in SWAN to allow for both sea state-dependent and frequency-dependent absorption characteristics emulating the behavior of WECs deployed in the ocean [7],[21]. A more in-depth review of SNL-SWAN's features is discussed in the following section.

SNL-SWAN and the TOMAWAC module differ in the approaches used to characterize the WEC. TOMAWAC uses hydrodynamic coefficients from a BEM to generate radiated and diffracted waves around a WEC. The hydrodynamics of the device are solved at each time step of the simulation. SNL-SWAN, including the meta-model approach proposed in this work, seeks to steer away from this approach. Rather, detailed data sets generated from an external high-fidelity time domain simulation are imported in the form of a look-up table. This method separates the domains of WEC developers and coastal modelers such that each group can apply its expertise. Additionally, preprocessed knowledge compiled from the simulator allows for fewer operations to be performed at each time step in SNL-SWAN further increasing the computational efficiency of any large scale coastal model. The time domain WEC simulation used to create the WEC SNL-SWAN meta-model is presented in the section "*Device simulations in the time domain*".

SNL-SWAN FUNCTIONALITY

SNL-SWAN characterizes a WEC using the standard method outlined in the IEC technical specifications [22] - the power matrix. A power matrix is a table of mechanical power (kW) produced by a WEC over a range of sea states characterized by a significant wave height (H_s) and an peak period (T_p). Relative capture width (RCW) curves [23] are tables which present a WEC's power absorption at different frequencies relative to the power in the wave. The user can choose one of these two representations as input into SNL-SWAN.

SNL-SWAN calculates the device's power absorption in two different ways. The method used is dependent on the input file and obstacle case specified by the user. When a power matrix is employed, the power in the variance density spectrum incident to an obstacle is found. The H_s and T_p are calculated from the incident spectrum. Bilinear interpolation is used to find the respective mechanical power absorbed for the corresponding sea state [23]. The power flux incident to the obstacle is then calculated using Equations 1 and 2.

$$P_{inc} = \int\int c_g E(\sigma,\theta) d\sigma d\theta \tag{1}$$

$$E(\sigma,\theta) = \frac{\rho g}{2} |\eta^2(\sigma,\theta)| \tag{2}$$

The mechanical power in the power matrix is normalized by the device width. The ratio of the incident wave flux from the convection term of the spectral wave equation, Equation 1, and the power production flux, Equation 2, is used to determine a transmission coefficient (K_t^2) [21] as seen in Equation 3. This coefficient is then applied at each grid point crossed by the WEC in the domain using Equation 4. The transmission coefficient (K_t^2) is used to characterize the device's energy absorption at that particular time step.

$$K_t^2 = \frac{P_{Lee}}{P_{Inc}} = 1 - \frac{P_{Abs}}{P_{Inc}} = 1 - RCW \tag{3}$$

$$\frac{\partial E}{\partial t} + c_{g,x}\frac{\partial K_t^2 E}{\partial x} + c_{g,y}\frac{\partial K_t^2 E}{\partial y} + c_{g,\theta}\frac{\partial E}{\partial \theta} + c_{g,\sigma}\frac{\partial E}{\partial \sigma} = S \tag{4}$$

The user has the option to use one of five different obstacle cases within the software suite.

Obstacle *case zero* corresponds to the standard obstacle command which extracts a certain percentage of the incident wave energy. A constant value is used across sea states and frequencies.

Obstacle case one uses a power matrix to calculate an effective transmission coefficient dependent on the sea state. The same coefficient is applied uniformly across all frequencies in the variance density spectrum [23].

Obstacle case two employs an RCW curve to calculate a constant transmission coefficient across all frequencies [23].

The peak frequency incident to the device is found within the RCW curve input by the user. Equation 6 is used to calculate K^2_t which is then applied uniformly across the wave spectrum incident to the device location.

Obstacle case three employs a power matrix to determine the transmission coefficient for each frequency bin in the incident energy spectrum. SNL-SWAN determines the H_s incident to the device. The row in the power matrix is then used as an RCW curve. A separate transmission coefficient is determined for each entry in the RCW curve and then applied to the respective frequency in the incident variance density spectrum [24].

Lastly, *obstacle case four* employs an RCW curve to determine K^2_t. The coefficient corresponding to each frequency in the curve is applied to the incident variance density spectrum. These values are not dependent on the incident sea state [23]. A more detailed description of each of the existing obstacles are present in the SNL-SWAN User Manual available on the SNL-SWAN website [21].

NOVEL OBSTACLE CASE FIVE

The standard methods used to characterize WECs such as power matrices and RCW curves are primarily used by developers to calculate the annual energy production of an isolated device. By applying a transmission coefficient calculated from the ratio of the incident power and mechanical power from a power matrix, as previously done in *obstacle case one*, it is assumed that any effect the device may have on the surrounding sea state is caused solely by the mechanical power extracted by the device. In short, by using this pre-existing parameterization, perfect conversion from incident to mechanical power is assumed and the energy removed from the environment is grossly underestimated. *Obstacle case five* seeks to remedy this oversight by creating a second input matrix which quantifies the total energy extracted from the incident wave spectrum by the device.

The total power extracted by a device is a sum of both the mechanical power recovered by the device and hydrodynamic losses. Power is dissipated by drag due to turbulence and viscosity, heat losses in the mechanical and electrical systems of the power take-off (PTO) and mooring drag, among other things. The premise of obstacle *case five* is that the energy lost by the incident waves to the WEC device can be calculated by totaling the energy extracted by the PTO and all hydrodynamic losses in the WEC system, as seen in Figure 1.

To calculate these energy sinks, an external time domain simulator, ProteusDS, is used to simulate WEC operations in irregular wave conditions. The simulator includes hydrodynamics forces alongside a finite element lumped mass mooring model, buoyancy calculations and PTO forces to calculate the multi degree of freedom motions. Power is calculated through the projection of the aforementioned forces by their state information. The energy flux inputs – Froude Krylov, diffraction, radiation and the drag inducing motion on the device are then used to generate the incident energy flux. The energy flux inputs are equivalent to the energy flux outputs, as seen in Figure 1. The incident energy flux exerted on a device is calculated for each sea state is then input by the user in a Power-with-losses matrix (PWLM).

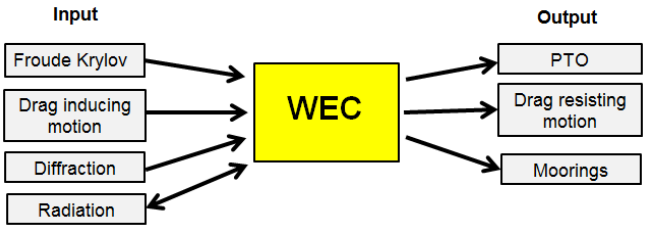

Figure 1: The incoming and outgoing energy flux of the WEC. The input parameters are used to generate a transmission coefficient for the device in the *obstacle case five* representation of the WEC.

Obstacle case five is equipped to calculate both the mechanical power produced by a device and the environmental impact associated with the device's operation. Two transmission coefficients are calculated. The traditional power matrix used in *obstacle case one* and *three*, is used to determine the mechanical power produced by a device. This value is output to the user. A second transmission coefficient is calculated using the novel PWLM. The ratio between the energy incident to the WEC and total extracted power is used to generate a transmission coefficient which is applied to the wave spectrum as it crosses an obstacle increasing the far field impact the device has on the sea.

Table 1 illustrates the differences between the pre-existing modules and the novel module.

Table 1: Obstacle case summary

Obstacle	User Input	Transmission
0	Percentage	Constant
1	Power Matrix	Constant
2	RCW Curve	Constant
3	Power Matrix	Frequency Dependent
4	RCW Curve	Frequency Dependent
5	Power Matrix PWLM	Constant

DEVICE DESCRIPTION

The performance of a Backwards Bent Duct Buoy (BBDB) oscillating water column (OWC) featured in the Department of Energy's Reference Model Project [25] was investigated in this study. The OWC has an internal air chamber and oscillating water column with a rigid exterior hull. The turbine inside the device is driven by a pressure differential created by the relative pressure between the air chamber and external environment [2].

The device is 27 metres wide and has a total mass of 2.03×10^6 kilograms. Additional device dimensions are presented in Figure 2.

DEVICE SIMULATIONS IN THE TIME DOMAIN

The device was simulated in WAMIT, a BEM code used to solve for radiation and diffraction in offshore structures [26]. The hydrodynamic and hydrostatic parameters found in WAMIT were later input into ProteusDS. ProteusDS is a time domain simulation package that was been experimentally validated for WECs [1], [27]. The simulation includes a six DOF floating OWC with the water elevation within the air chamber represented as an additional one DOF light piston. The hydrodynamic excitation, radiation, viscous drag and buoyancy are calculated for both bodies. A detailed and realistic mooring system is included.

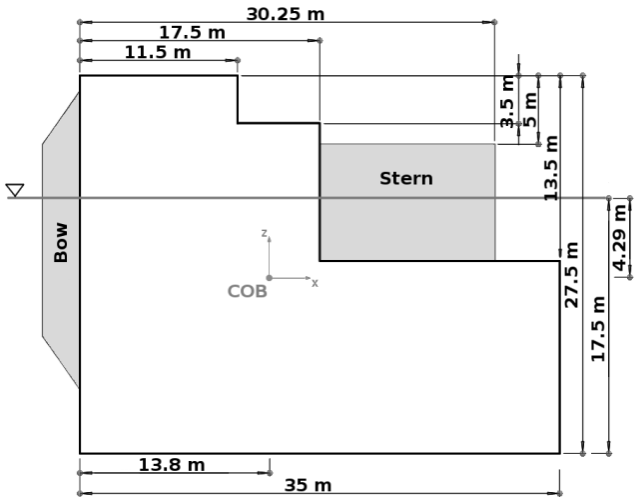

Figure 2: Dimensions of the BBDB OWC Reference Model [2]

The origin of each of the aforementioned components is outlined below. The excitation force corresponds to the dynamic pressure across the stationary body from the incoming wave and the resulting diffracted wave. The mooring forces are calculated using a cubic-spline lumped mass cable model presented by Buckham [28]. Finally, viscous drag is calculated by finding the total viscous drag force on each panel of the OWC's mesh based on Morrison's equation, for each translational degree of freedom. The energy corresponding to the Froude-Krylov, diffraction, radiation and motion inducing drag is responsible for the device's hydrodynamic response, as seen in Figure 1.

The device was modelled in 44 sea states. These sea states were chosen based on their occurrence at Amphitrite Bank (48.88N, 125.62W), a promising WEC installation location off the west coast of Vancouver Island [29]. The sea state power histogram in Figure 3 presents the most prevalent sea states at Amphitrite Bank. Sea states were only modelled if they occurred for more than 24 hours over the course of the year in order to reduce the computational expense of these simulations. Additional sea states were simulated on the edges of the bins in Figure 3 to accommodate limitations in the SNL-SWAN power interpolation routine.

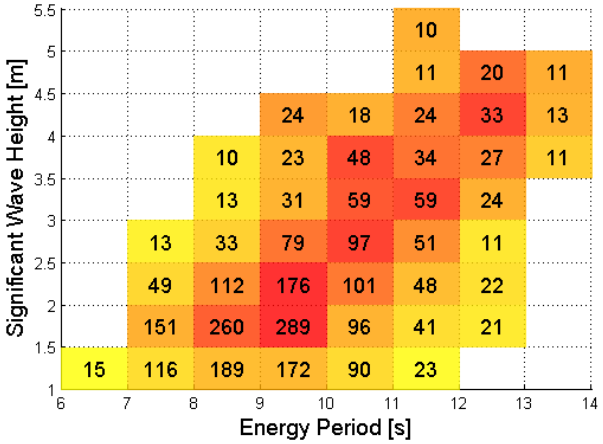

Figure 3: Number of times each sea state occurred at Amphitrite Bank in 2006 at a three hour resolution. Sea states that occurred for less than 24 hours (eight time steps) have been truncated.

Each sea state was simulated in ProteusDS using a Pierson-Moskowitz spectrum which closely resembles the wave resource at this location [30]. A cosine squared directional spread, following DNV [31], is used. For each sea state, the simulation was run for 20 minutes, as recommended by IEC [22] with 140 different wave segments [32]. An image of the device and the accompanying mooring can be seen in Figure 4.

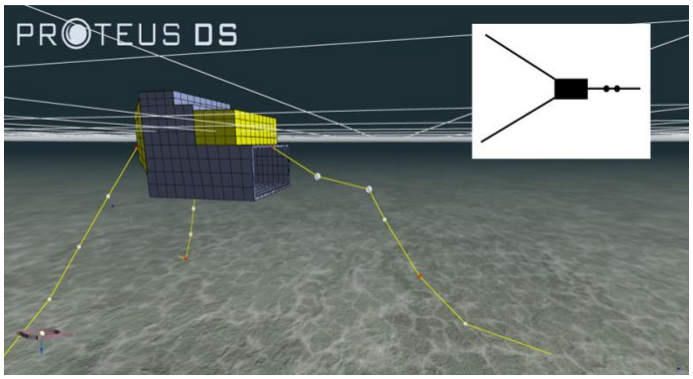

Figure 4: OWC and mooring depiction in ProteusDS

POWER MATRIX GENERATION

The power matrix for the OWC was generated by finding the mechanical power generated by the device in each sea state presented in Figure 5. The PWLM presented in Figure 6 includes the total power extracted by a device from the incident wave energy spectrum. This energy flux is a sum of: the mechanical power produced by the device, the losses from moorings, and motion-resisting viscous drag, which are equivalent to the incident energy flux, as previously described in Figure 1.

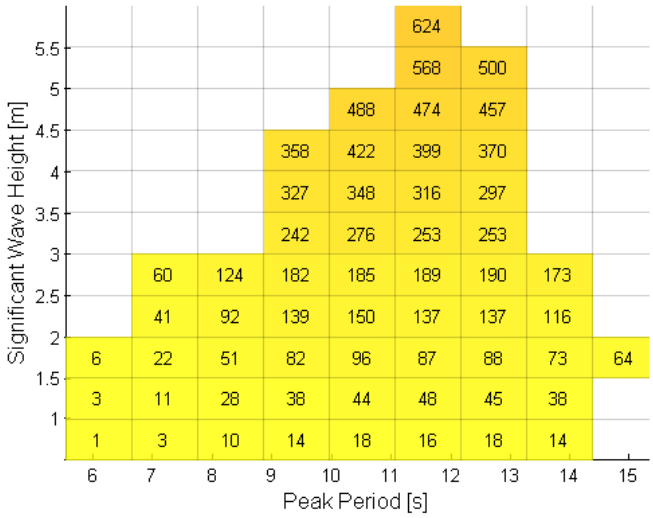

Figure 5: Mechanical power (kW) produced by the OWC for each sea state

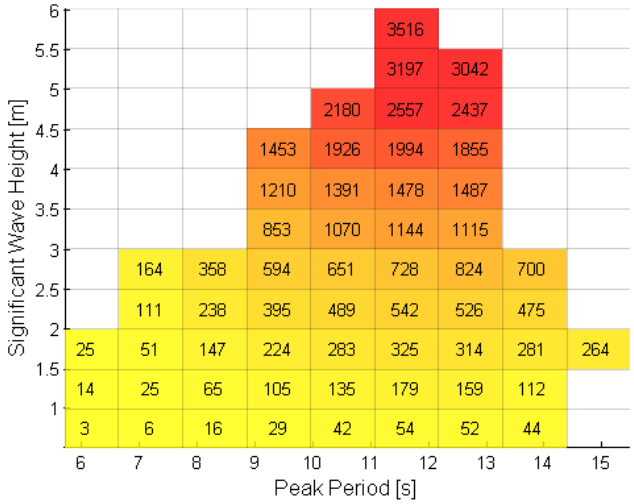

Figure 6: Power extracted (kW) by device including hydrodynamic losses

DEVICE SIMULATIONS IN SNL-SWAN

Two device configurations were run in SNL-SWAN to demonstrate the effectiveness of the novel device parameterization. The first configuration examines the impact a single device has on the surrounding wave climate when a traditional power matrix is employed and when hydrodynamic losses are also considered. The device's impact on the H_s of the surrounding wave climate is investigated in the most commonly occurring sea state at Amphitrite Bank (H_s=1.75 m, T_p =11.1 s) as seen in Figure 3. The second configuration is comprised of two devices in series. This configuration is analyzed to both quantify the devices' environmental footprint and to investigate the impact a device's shadow has on a subsequent device's power production. A 200 metre separating distance was chosen for both practical reasons and recommendations from previous papers. This distance would provide maintenance vessels with sufficient space for operation and sufficient distance for the watch circle. Secondly, separating distances of 100 metres to 200 metres are recommended for devices 10-20 metres wide to reduce negative interactions [33]. Results from 44 sea states were compared between *obstacle cases one* and *five* resulting in a total of 88 simulations. The power extracted from the sea and mechanical power produced by both devices was recorded and compared in both *obstacle case one* and *five*.

Both configurations were run in a flat bottom Cartesian domain with a grid resolution of 10 meters in the x and y directions and a uniform 50 meter depth. The first device was centered at (1215 m, 1215 m). The second device was placed 200 metres directly behind the first at (1415 m, 1215 m). A Pierson Moskowitz spectrum characterized with an H_s, T_p and directional spreading was across the model domain in each of the test cases. Wind growth, triad and quadruplet wave interactions were disabled for this simulation to better demonstrate the impact the device has on the surrounding sea.

RESULTS

This work aims to quantify the environmental impact a device has on the surrounding sea more accurately and to illuminate how considering hydrodynamic losses can change the annual power production estimates for different devices in an array. Environmental impact is quantified by analyzing the change in H_s across the computational domain for one and two devices. Power production is analyzed by comparing the power produced from a device both on a sea state basis and over the course of a year.

ENVIRONMENTAL IMPACT

The importance of including hydrodynamic losses in the representation of a WEC is investigated in relative percent differences and in absolute terms. Figure 7 presents contours corresponding to the percent difference in signficant wave height in the lee of a device when modelled using a traditional power matrix and a matrix accounting for losses.

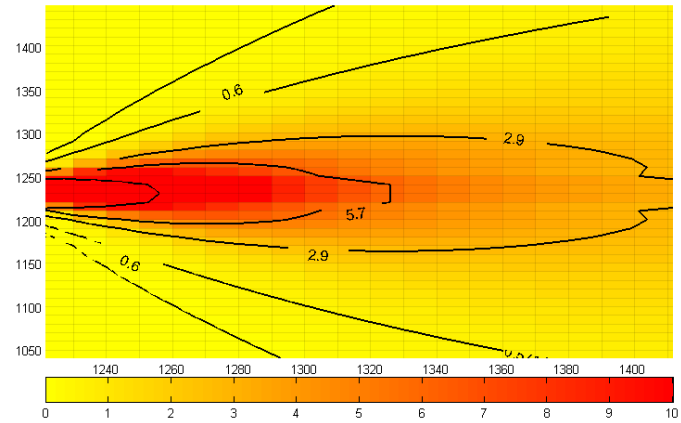

Figure 7: Percent difference in Hs observed in the lee of a single device when accounting for hydrodynamic losses in an H_s = 1.75 m and T_p=11.1 s sea state.

The inclusion of hydrodynamic losses in a device's representation within SNL-SWAN increases the amount of energy extracted from the incident waves. The inclusion of these losses is most pronounced up to 100 metres behind the device where a 5.7% decrease in H_s can be observed. Further to the east of the device, spectral action density diffuses into the lee of the device, closely approximating diffraction and decreasing the relative difference between obstacle case one and five. A 2.9% difference in H_s can be observed between the two obstacle cases 200 metres behind the device,

Figure 8 presents the extent of two devices' impact on the surrounding wave climate when obstacle cases one and five are employed. In obstacle case one, the incident H_s is reduced by 0.4 metres up to 200 metres away from the device. The decrease in H_s is exacerbated in obstacle case five where the 0.4 metre decrease in H_s is observed 600 metres behind the shadowed device. The more prominent decrease in H_s is attributed to the residual impact of the first device on the sea.

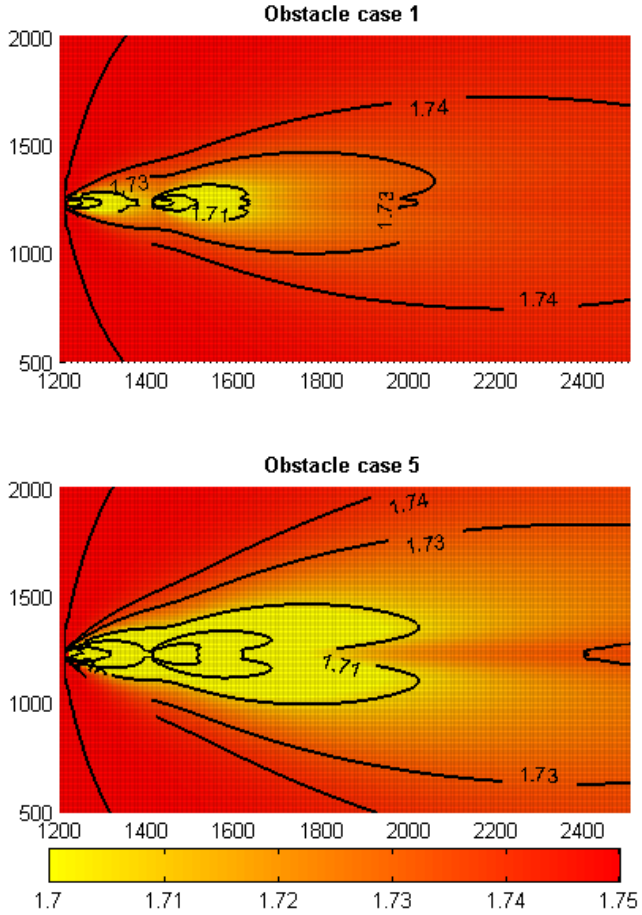

Figure 8: Change in significant wave height in the lee of two OWC devices 200 metres apart. The first device is located at (1215, 1215) and the second device is located at (1415, 1215).

Results presented in Figure 7 and Figure 8 will vary between sea states. Variations can be attributed to how efficiently a device operates in each sea, the proximity between devices, and finally, the number of devices arranged in series.

The recovery distance of the incident H_s in the lee of two devices is investigated in Figure 9. A sharp decrease in H_s is observed directly in the lee of both devices. In obstacle case one, the H_s is initially reduced to 82% of its original value. The H_s recovers to 98% of its original height and is then reduced to 80% in the lee of the second device. The power extracted by the device in obstacle case five results in a reduction to 44% of the incident H_s. The recovery in H_s in the lee of obstacle case five is relatively quicker given the drastic difference in H_s reduction directly behind the device. In this sea state, obstacle case five requires 2.6 times the distance obstacle one requires to recover to 95% of the incident H_s.

The inclusion of hydrodynamic losses in the investigation of environmental impact is paramount. Obstacle case five resulted in an average 5.6% decrease in H_s up to 100 metres behind the device over 44 sea states. In addition, obstacle case five requires over twice the distance obstacle case one needs to recover to 95% of the incident H_s. The reduction in H_s is assumed to compound as more devices are placed in series.

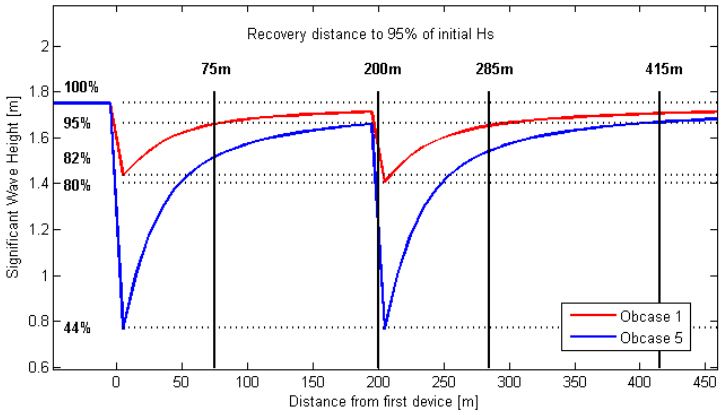

Figure 9: Cross sectional view of the Hs recovery behind two BBDB OWCs. The percentage of incident Hs is indicated with dotted lines. The distances associated with a 95% Hs recovery for obstacle cases one and five is presented with solid lines.

POWER PRODUCTION

The amount of mechanical power produced by the first device in series is identical in *obstacle cases one* and *five*. Differences in power produced are more pronounced in shadowed devices where reduced incident energy is observed. The decrease in power production of the shadowed device is analyzed by sea state, as in Figure 10 and in terms in annual power production. The decrease in mechanical power produced by a device 200 metres behind the first device varies from sea state to sea state.

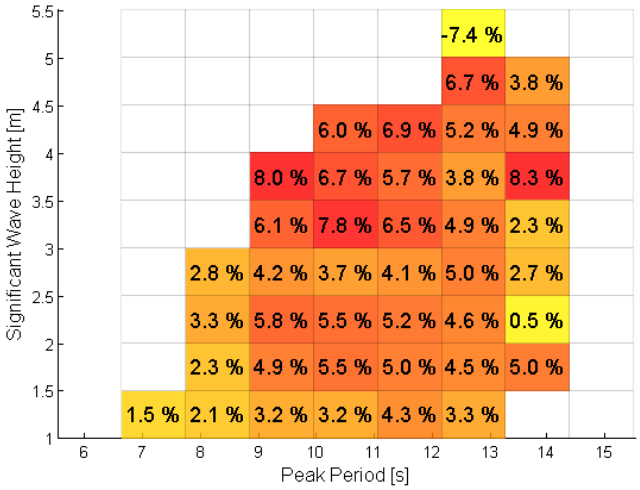

Figure 10: Decrease in mechanical power produced by the second device when employing obstacle case five opposed to obstacle case one.

In general, the largest differences in performance between the two obstacle cases are observed where the BBDB OWC's variable frequency drive is the most efficient (H_s=2.75 m , T_p=9.4 s) [2]. In higher energy seas, losses can be attributed to a number of phenomena. For one, drag increases proportionally to the square of the device's velocity which increases in higher energy sea states. Secondly, moorings limit the device's motion in high energy seas, hindering power production. An outlying data point can also be observed in the H_s=5.25 m and T_p= 12.7s. In this particular area of the power matrix, there is a positive gradient in power absorption the lower the significant wave height. When *obstacle case five* is employed, the H_s in the lee of the first device is lowered to a point where the second device references a transmission coefficient correlating to a more efficient sea state bin. This phenomenon ultimately results in the shadowed device producing more power when *obstacle case five* is employed. It should be noted that this may be an artificial increase in power given the turbine speed for this bin was interpolated in previous works [2]. The WEC metamodel linearly interpolates transmission coefficients from a power matrix. Given the power production and power absorption of a device is non-monotonic due to the non-linearities in the time domain model, small decreases in H_s may shift a device's transmission coefficient to a neighboring sea state bin. An anomalous result can also be observed in the H_s=3.75 m and T_p=13.8s bin for similar reasons. The turbine speed for this bin was interpolated as per the methodology in Bailey et al. [2]. The device's performance in the time domain model may have been reduced relative to other sea states, causing an artificial difference in these results.

The maximum decrease in power produced by the second device when obstacle case one is employed occurred in H_s=1.75 m and T_p=9.4 s, which is the sea state in which the device is the most efficient [2]. In the case of obstacle case five, the maximum decrease in power produced was observed in H_s=3.75 m and T_p=9.4 s, which corresponds to the sea state in which the most hydrodynamic losses occur.

To quantify the importance of these findings on a larger scale, the influence of the hydrodynamic losses was investigated on the second device's annual power production. The annual power production was calculated by multiplying the power produced in each sea by the number of times each sea state occurred on Amphitrite Bank in 2006. Over the course of a year, the power produced by the shadowed device was overestimated by 4.5% when *obstacle case one* was employed, as seen in Table 2. The annual power production of the first device in both obstacle cases was 299 MW. The shadowed device in *obstacle case one* produced 98% of the power produced by the first device. *Obstacle case five* produced only 93.7% of the power produced by the first device. Overall, the inclusion of hydrodynamic losses has a large impact on the power produced on shadowed devices.

Table 2: Annual power production of the shadowed device as calculated using obstacle cases one and five

	Obstacle case		Percent Decrease
	One	*Five*	
Total Power [MW]	293	280	4.5

CONCLUSIONS

Quantifying the environmental impact of a WEC and calculating the power produced from an array are difficult to address. SNL has created a modified version of SWAN in which the user can parameterize a device using a power matrix or relative capture width curve [23]. The sea state and frequency-specific characterization of devices has largely improved the fidelity of WEC representations in spectral models. Representing devices in a wave field by mechanical power extracted alone however, is insufficient to gain a holistic understanding of the device's impact on the surrounding wave climate. The contributions of this work are twofold. The first corresponds to the generation of a PWL matrix for the BBDB OWC device to characterize the impact the device has on the surrounding wave field. The second contribution lies in the development of a novel obstacle case which allows the user to assimilate power performance and hydrodynamic data from external time domain simulations into a spectral model. Two configurations of devices were run in 44 sea state simulations.

The environmental impact of the device was quantified by decreases in H_s. Obstacle case five resulted in an average 5.6% decrease in H_s up to 100 metres behind the device over 44 sea states. The difference between the H_s of the two obstacle cases decreased as waves propagated further away from the device. Obstacle case five recovered to 95% of the incident H_s over 2.6 times the distance required by obstacle case one for the same sea state.

The power produced by the shadowed device was also investigated. On a sea state basis, a mean decrease of 4.5% was observed when employing obstacle case five. Over the course

of a year, the power produced by the shadowed device would be overestimated by 4.5% if obstacle case one were employed for this analysis. It is expected that as the number of devices in series increases, both the reduction in H_s will be exacerbated and the annual power produced by each device in series will also decrease due to the reduction in incident wave energy.

LIMITATIONS

The work presented aims to extract phase resolved WEC hydrodynamics in a time domain simulation, package them in a pre-compiled meta-model, and apply that meta-model within SNL-SWAN driven analyses of WEC farm operations. The current study aims to reveal the sensitivity of the SNL-SWAN outputs to the particular meta-model structure. Given the increased fidelity of the WEC meta-model included in this work, realized through the pre-processed time domain simulation data, the authors propose that the changes in SNL-SWAN output reported in this work do represent improvements. However, the proposed framework is yet to be validated with experimental and field trial data.

The proposed framework is subject to the fundamental limitation of the phase-averaged nature of SWAN. The model cannot explicitly model phenomena such as radiation and diffraction which are critical in calculating the wave field around a farm. However, SWAN's diffraction approximation has been validated, and a similar numerical approximation may be implemented in the future for radiation. Finally, radiation is presently represented as a bulk change in the transmission coefficient mechanism. As a result, the radiation manifests itself only in the lee of the WEC, which does not accurately represent this particular phenomenon. Improvements to the radiation representation will be addressed further in the following section.

FUTURE WORK

The modifications implemented in SNL-SWAN aid in both predicting power production and environmental impact of a WEC array. Future work will stem in two directions. Firstly, further testing and application of the aforementioned *obstacle case* will be conducted. Larger array configurations will be implemented in desirable locations off the West Coast of Vancouver Island. Annual power can then be computed directly in SNL-SWAN through a nonstationary hindcast simulation.

Secondly, the assimilated WEC representation will be improved. A more realistic representation of radiation will be implemented by modifying the existing reflection command within SNL-SWAN. A frequency-dependent *obstacle case* similar to *obstacle cases three* and *four* is also currently under development.

ACKNOWLEDGMENTS

This work was funded by Natural Resources Canada, the Pacific Institute of Climate Solutions, the Natural Sciences and Engineering Research Council of Canada and Ocean Networks Canada.

REFERENCES

[1] R. S. Nicoll, C. F. Wood, and A. R. Roy, "Comparison of Physical Model Tests With a Time Domain Simulation Model of a Wave Energy Converter," in *ASME 2012 31st International Conference on Ocean, Offshore and Arctic Engineering.*, 2012.

[2] H. Bailey, B. R. D. Robertson, and B. J. Buckham, "Wave-to-Wire Simulation of a Floating Oscillating Water Column Wave Energy Converter." 2016.

[3] A. Combourieu, M. Lawson, A. Babarit, K. Ruehl, A. Roy, R. Costello, P. L. Weywada, and H. Bailey, "WEC 3 : Wave Energy Converter Code Comparison Project," pp. 1–10, 2015.

[4] S. J. Beatty, M. Hall, B. J. Buckham, P. Wild, and B. Bocking, "Experimental and numerical comparisons of self-reacting point absorber wave energy converters in regular waves," *Ocean Eng.*, vol. 104, pp. 370–386, 2015.

[5] M. Pe, G. Giorgi, and J. V Ringwood, "A Review of Non-Linear Approaches for Wave Energy Converter Modelling," no. 1, pp. 1–10, 2015.

[6] M. Pe, J. Gilloteaux, and J. V Ringwood, "Nonlinear Froude-Krylov force modelling for two heaving wave energy point absorbers," pp. 1–10, 2015.

[7] K. Ruehl, A. Porter, A. Posner, and J. Roberts, "Development of SNL-SWAN , a Validated Wave Energy Converter Array Modeling Tool," *Proc. 10th Eur. Wave Tidal Energy Conf., Aalborg, Denmark*, 2013.

[8] K. E. Silverthorne and M. Folley, "A New Numerical Representation of Wave Energy Converters in a Spectral Wave Model."

[9] M. Folley, A. Babarit, B. F. M. Child, D. Forehand, L. O'Boyle, K. Silverthorne, J. Spinneken, V. Stratigaki, and P. Troch, "A Review of Numerical Modelling of Wave Energy Converter Arrays," in *ASME 2012 31st International Conference on Ocean, Offshore and Arctic Engineering*, 2012, pp. 1–12.

[10] P. Ricci, J. Saulnier, and A. F. D. O. Falcão, "Point-absorber arrays : a configuration study off the Portuguese West-Coast."

[11] G. D. B. M. Vantorre, C. B. J. De Rouck, and P. Frigaard, "Power absorption by closely spaced point absorbers in constrained conditions," vol. 4, no. November 2009, pp. 579–591, 2010.

[12] V. Venugopal and G. H. Smith, "Wave climate investigation for an array of wave power devices."

[13] C. Beels, P. Troch, K. De Visch, J. P. Kofoed, and G. De Backer, "Application of the time-dependent mild-slope equations for the simulation of wake effects in the

lee of a farm of Wave Dragon wave energy converters," *Renew. Energy*, vol. 35, no. 8, pp. 1644–1661, 2010.

[14] C. Beels, P. Troch, G. De Backer, M. Vantorre, and J. De Rouck, "Numerical implementation and sensitivity analysis of a wave energy converter in a time-dependent mild-slope equation model," *Coast. Eng.*, vol. 57, no. 5, pp. 471–492, 2010.

[15] V. Stratigaki, "Experimental Study and Numerical Modelling of Intra-Array Interactions and Extra-Array Effects of Wave Energy Converter Arrays Vasiliki Stratigaki," 2014.

[16] A. Babarit, M. Folley, F. Charrayre, C. Peyrard, and M. Benoit, "On the modelling of WECs in wave models using far field coefficients," *Eur. Wave Tidal Energy Conf. EWTEC*, pp. 1–9, 2013.

[17] L. Holthuijsen, *Waves in Oceanic and Coastal Waters*. Delft: Cambridge University Press, 2007.

[18] L. H. Holthuijsen, A. Herman, and N. Booij, "Phase-decoupled refraction – diffraction for spectral wave models," vol. 49, pp. 291–305, 2003.

[19] D. L. Millar, H. C. M. Smith, and D. E. Reeve, "Modelling analysis of the sensitivity of shoreline change to a wave farm," *Ocean Eng.*, vol. 34, no. 5–6, pp. 884–901, 2007.

[20] H. C. M. Smith, C. Pearce, and D. L. Millar, "Further analysis of change in nearshore wave climate due to an offshore wave farm: An enhanced case study for the Wave Hub site," *Renew. Energy*, vol. 40, no. 1, pp. 51–64, 2012.

[21] A. Porter, K. Ruehl, and C. Chartrand, "Further Development of Snl - Swan , a Validated Wave Energy Converter Array Modeling Tool," *2nd Mar. Energy Technol. Symp.*, pp. 1–9, 2014.

[22] IEC, "TC114: Marine energy - Wave, tidal and other water current converters - Part 100: Electricity producing wave energy converters - Power performance assessment," IEC/TS 62600-100 Ed. 1.0, 2012.

[23] K. Ruehl, C. Chartrand, and A. K. Porter, "SNL-SWAN User's Manual," 2014.

[24] C. Chartrand and K. Ruehl, "Personal Communication." 2015.

[25] U.S DOE, "Reference Model Project (RMP)," 2014. .

[26] WAMIT Inc., "WAMIT User Manual Version 7," 2013.

[27] P. B. Garcia-Rosa, R. Costello, F. Dias, and J. V Ringwood, "Hydrodynamic Modelling Competition - Overview and Approaches," in *ASME 2015 34th International Conference on Ocean, Offshore and Arctic Engineering*, 2015.

[28] B. J. Buckham, "Dynamics modelling of low-tension tethers for submerged remotely operated vehicles," University of Victoria, 2003.

[29] B. Robertson, C. E. Hiles, E. Luczko, and B. J. Buckham, "Quantifying the Wave Power and Wave Energy Converter Array Production Potential," *Int. J. Mar. Energy*, vol. 1, 2016.

[30] B. Robertson, H. Bailey, D. Clancy, J. Ortiz, and B. Buckham, "Influence of wave resource assessment methodology on wave energy production estimates," *Renew. Energy*, vol. 86, pp. 1145–1160, 2016.

[31] DNV, *Recommended practice DNV-RP-C205 environmental conditions and environmental loads*. 2010.

[32] DNV, "Recommended Practice. DNV-RP-H103. Modelling and Analysis of Marine Operations," 2011.

[33] a. Babarit, "On the park effect in arrays of oscillating wave energy converters," *Renew. Energy*, vol. 58, pp. 68–78, 2013.